# Novel Broadband Cavity-Enhanced Absorption Spectrometer for Simultaneous Measurements of NO2 and Particulate Matter

Gaoxuan Wang, Lingshuo Meng, Qian Gou, Benjamin Hanoune, Suzanne Crumeyrolle, Thomas Fagniez, Cécile Coeur-Tourneur, Rony Akiki, Weidong Chen

# A Novel Broadband Cavity-Enhanced Absorption Spectrometer for Simultaneous measurements of NO$_2$ and particulate matter

Gaoxuan Wang,[1,2] Lingshuo Meng,[2] Qian Gou,[*,3] Benjamin Hanoune,[4] Suzanne Crumeyrolle[5], Thomas Fagniez,[2] Cécile Coeur,[2] Rony Akiki,[6] Weidong Chen[*,2]

[1]Ningbo research institute, Zhejiang University, Qianhu south road Rd.1, 315100 Ningbo, China;

[2]Laboratoire de Physicochimie de l'Atmosphère, Université du Littoral Côte d'Opale, 189A Avenue Maurice Schuman, 59140 Dunkerque, France

[3]School of Chemistry and Chemical Engineering, Chongqing University, Daxuecheng South Rd. 55, 401331 Chongqing, China.

[4]Physicochimie des Processus de Combustion et de l'Atmosphère, Université Lille1 Sciences et Technologies, Bâtiment C11, 59655 Villeneuve d'Ascq, France.

[5]Laboratoire d'Optique Atmosphérique, Université de Lille1, Bâtiment P5, 59655 Villeneuve d'Ascq, France.

[6]ENVEATM (ex Environment SA), 111 Boulevard Robespierre CS 80004, 78304 Poissy Cedex 4, France

**ABSTRACT:** A novel instrument based on broadband cavity enhanced absorption spectroscopy has been developed using a supercontinuum broadband light source, which showcases its ability in simultaneous measurements of the concentration of NO$_2$ and the extinction of particulate matter. Side-by-side intercomparison was carried out with the reference NOx analyzer for NO$_2$ and OPC-N2 particle counter for particulate matter, which shows a good linear correlation with $r^2 > 0.90$. Measurement limits (1σ) of the developed instrument were experimentally determined to be 230 pptv in 40 s for NO$_2$ and 1.24 Mm$^{-1}$ for the PM extinction in 15 s, respectively. This work provides a promising method in simultaneously monitoring atmospheric gaseous compounds and particulate matter, which would further advance our understanding on gas-particle heterogeneous interactions in the context of climate change and air quality.

Atmospheric composition, including trace gases and particulate matter (PM), can have warming or cooling effects on climate through regulating the solar radiation in the atmosphere,[1] or aggravate air pollution through a complex series of chemical and physical transformations.[2] Long-term exposure to high concentration of air pollutants including PM, NO$_2$, NO, etc, can cause direct or indirect damage to the human health and increases risk of respiratory and lung diseases.[3,4] Many atmospheric PM are generated by gas-to-particle conversions (e.g., nucleation, condensation) to be formed as secondary organic aerosol causing severe air pollution.[5] Therefore, simultaneous measurements of atmospheric gaseous compounds and PM can largely advance our understanding on climate-atmosphere chemistry and gas-particle heterogeneous interactions and be of great interest for air quality monitoring.[1-6]

Simultaneous detection of gas and PM usually requires multiple instruments or a single instrument with complex structure due to different chemical or physical properties between gas and PM. Individual measurements of gas and PM using multiple instruments generally require more sensors with high cost and large volume and is not suitable for field campaign. Single instrument for simultaneous measurement of gas and PM is highly required and also challenging. Spectroscopy is a common analytical method and has been widely used for monitoring atmospheric gas or

PM, separately. Spectroscopy-based gas sensing is becoming more popular and mature with advantages of high sensitivity and selectivity.[7,8] However, spectroscopy-based PM sensing is challenging, as the spectral signal of PM highly depends on PM parameters such as its size distribution, mixing state, and morphology.[9,10] Routine optical techniques for PM measurements include: (1) nephelometry for the scattering measurement of PM;[11] (2) filter-based method[12]or photoacoustic spectrometry (PAS)[13-15] for the absorption measurement of PM; (3) Long-path absorption approaches involving multipass cell[16,17] or cavity enhanced absorption spectrometry (CEAS)[7] for the extinction measurement of PM. Nephelometry and filter-based methods are not adaptable for gas measurement, prohibiting the further realization of the simultaneous measurement of gas and PM. Photoacoustic spectrometry is based on photo-acoustic (PA) effect converting the absorbed photon energy into acoustic sound.[15] However, the PAS method cannot distinguish the acoustic signal resulting from gas or PM as the absorbed optical energy by gas or PM absorption is identical and can be transferred to the surrounding air to generate acoustic signal.[18,19] The sensitivity achieved by the multipass cell measurement is generally limited due to its relatively short optical absorption path length.[20]

The CEAS approaches have drawn considerable attention, which has been widely used since last decades for the measurements of aerosol extinction with a detection limit less than 1 Mm$^{-1}$, including cavity ring-down spectroscopy (CRDS),[21] cavity attenuated phase shift spectroscopy (CAPS),[22] and incoherent broad band cavity enhanced absorption spectroscopy (IBBCEAS).[23,24] Indeed, taking advantage of the high finesse optical cavity, CEAS can have a rather low limit of detection required by field measurements, through an effective absorption path-length up to several kilometers.[7,21-24] The CRDS method using a narrow bandwidth laser [25] and the CAPS method using LED (light emitting diode) [26] could not provide the ability of simultaneous quantification of gas absorption and PM extinction. Broadband IBBCEAS measurements allow simultaneous quantification of multiple species using a broad-band light source providing abundant spectral information. Simultaneous measurements of $NO_2$ and PM have been demonstrated by differentiating rapid variation of spectral signal resulting from gas absorption and slowly varying spectral signal due to the PM extinction.[23,27,28] In their experiment, the instrumental baseline was not, however, real-time checked which might give rise to a large uncertainty when measuring small PM extinction. [29]

Taking $NO_2$ and PM as the target species, herein, a novel spectroscopic instrument of broadband cavity enhanced absorption spectroscopy (BBCEAS) using a supercontinuum (SC) broadband light source has been developed for simultaneous measurements of the $NO_2$ concentration and PM extinction, which can present a high correlation ($r \sim 0.7$–0.96) in the polluted environments.[6] The SC light offers laser-like output properties which allows a significant improvement of the light-cavity coupling efficiency, with exceptional advantages of high brightness and broad spectral coverage. The BBCEAS instrumental baseline was regularly checked to remove any drift caused by adverse factors in the light source or photodetectors, as well as resulted from any environmental fluctuations which allows significantly improvement in the measurement accuracy of PM extinction coefficient and the $NO_2$ concentration. Measurement limits ($1\sigma$) of the developed BBCEAS instrument were experimentally determined to be 230 pptv in 40 s for $NO_2$ and 1.24 Mm$^{-1}$ for the PM extinction in 15 s, respectively.
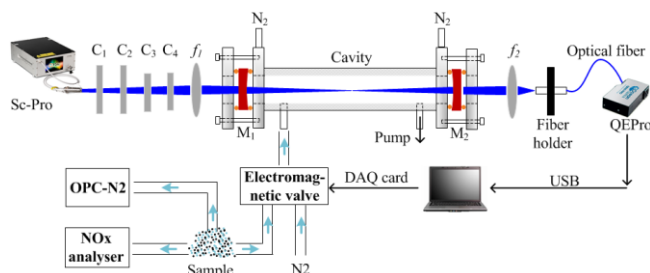
## EXPERIMENTAL SECTION



**Figure 1** Schematic of the BBCEAS instrument developed in the present work. A NOx analyzer (Environment SA, AC-31 M) and an optical particle counter (OPC-N2, Alphasense) were used for side-by-side inter-comparison measurements of $NO_2$ and PM. SC-Pro: supercontinuum source; $M_1$, $M_2$: high reflectivity mirror; QEPro: spectrometer; $C_1$, $C_2$: optical attenuators; $C_3$, $C_4$: optical filters; $f_1$, $f_2$: focusing lens.

**Instrumentation.** The schematic of the developed broadband cavity enhanced absorption spectrometer is presented in Figure 1. A fiber pigtailed supercontinuum light (SC-Pro, YSL Photonics, 410~2400 nm, up to 4 W) was filtered to provide a broadband radiation over the spectral region of 440-460 nm where both $NO_2$

and PM exhibit strong absorptions.[15] The used supercontinuum source SC-Pro provides a quasi-continuous light with a repetition rate of 25 MHz. The selected SC radiation (1.84 mW) was then focused by a plano-convex lens ($f_1$ = 200 mm) and injected into a high finesse optical cavity. Two spherical mirrors (0.5" diameter, 1 m radius of curvature, Layertec) with reflectivity > 99.99% around 450 nm were used as mirrors of the BBCEAS cavity with a physical cavity length of $d$ = 20.5 cm, which results in an optic path length of 4.1 km and a cavity lifetime of 13.67 μs. The period of the light pulse emitting from the supercontinuum source is far shorter than the cavity lifetime and the light source repetition rate will not influence the system response. The cavity material is stainless steel, which is used to minimize the losses of PM[30] and $NO_2$[31]. The emergent light from the cavity was measured with a grating spectrometer (QEPro, Ocean Optics, with 0.53 nm spectral resolution covering 290 - 480 nm) through lens $f_2$ (= 100 mm) and a multimode optical fiber.

In order to avoid light saturation of the CCD detector of the spectrometer at the edges of high-reflectivity range of the cavity mirrors, a specific filter set was designed which consisted of two optical filters ($C_3$ and $C_4$) associated with two optical attenuators ($C_1$ and $C_2$) used to prevent optical filters from optical power damaging. C1 (Model FC10, Opton laser international) is used to remove the most part of light power at the infrared while C2 (Model C3C22, Opton laser international) prevents the optical power at wavelengths shorter than 425 nm. Filter C3 (FGS900, Thorlabs) with a bandpass 315-700 nm effectively attenuates the light in the infrared after passing through C1 and C2. Filter C4 (Band filter 86338, Edmund) is used to remove undesirable wavelengths from 465 to 725 nm at which the cavity mirror's reflectivity was low and the spectrograph might be saturated. The resulting transmission region used for the present work is then 440-460 nm (as shown in Figure S1 in the support information).

A NOx analyzer (AC-31 M, Environment S.A) and an optical particle counter (OPC-N2, Alphasense) were deployed for side-by-side inter-comparison measurements of $NO_2$ and PM (PM1, PM2.5, and PM10), respectively. An electromagnetic valve (Solenoid Valve 6014, Burkert) was used to switch the cavity inlet from pure $N_2$ for baseline measurement and from the air sample for measurement cycles at a flow rate of 0.4 L/min. The main valve material is stainless steel which will not cause any loss on PM and $NO_2$. A LabView program was developed to regularly check the background baseline and to process the BBCEAS measurement data.

**Measurement principle.** Broadband spectral information from BBCEAS spectra allows simultaneously quantifying the absorption of trace gas and the extinction of PM. It is achieved by separating the spectral structures into rapidly and slowly varying parts corresponding to gas absorption features and PM extinction associated with instrument baseline, respectively. In BBCEAS measurement approach, the gas absorption $\alpha_{abs.,gas}(\lambda)$ and aerosols extinction $\alpha_{ext.PM}(\lambda)$ from air samples can be determined through the following equation:[32-34]

$$\alpha_{abs.gas}(\lambda) + P(\lambda) = \left( \frac{1-R(\lambda)}{d} + \alpha_{Ray.N2}(\lambda) \right) \times \left( \frac{I_0(\lambda) - I(\lambda)}{I(\lambda)} \right) \quad (1)$$

where $I(\lambda)$ and $I_0(\lambda)$ are the transmitted light intensities with air samples and with nitrogen $N_2$ (for baseline) inside the cavity, respectively; $R(\lambda)$ is the mirror reflectivity, $d$ (cm) is the distance between two cavity mirrors and $\alpha_{Ray.N2}(\lambda)$ is the Rayleigh scattering coefficient of $N_2$. The $1^{st}$ term on the left-hand side $\alpha_{abs.,gas}(\lambda)$ is related to the gas absorption, based on the Lambert-Beer law:

$$\alpha_{abs.gas}(\lambda) = \sum_i n_i \times \sigma_i(\lambda) \qquad (2)$$

where $n_i$ and $\sigma_i$ are the number concentration and the reference cross section for the $i^{th}$ gas species, respectively. The 2$^{nd}$ term $P(\lambda)$ is a polynomial function used to account for the sum of PM extinction $\alpha_{ext.PM}(\lambda)$ and the spectral baseline $\alpha_{baseline}(\lambda)$:

$$P(\lambda) = \alpha_{ext.PM}(\lambda) + \alpha_{baseline}(\lambda) \qquad (3)$$

Based on the BBCEAS measurements, the concentration of trace gas $n_i$ and the aerosol extinction $\alpha_{ext.PM}(\lambda)$ can thus be simultaneously retrieved by fitting the experimental data (right-hand of Eq. (1)) to reference cross-section $\sigma_i(\lambda)$ and the polynomial function $P(\lambda)$, as followings: (1) the rapidly varying structured spectrum is fitted as a linear combination of the known absorbers cross section and the concentration of trace gas determined by nonlinear least-square fitting based on the Levenberg-Marquardt algorithm;[34] and (2) the slowly varying component of the spectrum $P(\lambda)$, including both the PM extinction and baseline variation, is determined by subtracting the structured gas absorption from the total measured optical attenuation. Figure 2 represents the time series measurement of wavelength-dependent PM extinction retrieved from the slow variation in the BBCEAS spectrum in which the instrumental baseline was regularly checked.
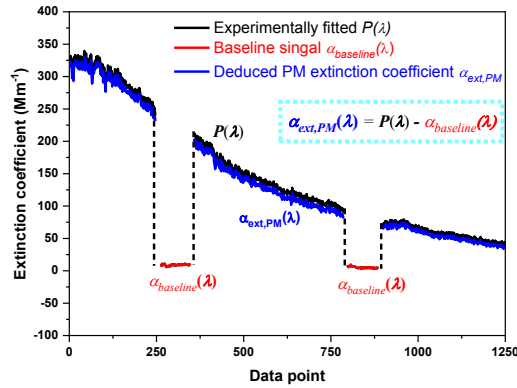


**Figure 2** Schematic of the principle of retrieving PM extinction at the wavelength of $\lambda$ from the slow variation in the BBCEAS spectrum. The fitted $P(\lambda)$ (black) is considered as the total contribution from $\alpha_{baseline}(\lambda)$ and $\alpha_{ext,PM}(\lambda)$ when the sampled air is inside the cavity, and $P(\lambda)$ equals to $\alpha_{baseline}(\lambda)$ when only pure $N_2$ is inside the cavity for the baseline measurement. The extinction coefficient $\alpha_{ext,PM}(\lambda)$ of PM in the air sample is thus deduced from $\alpha_{ext,PM}(\lambda) = P(\lambda) - \alpha_{baseline}(\lambda)$.

**Calibration of the mirror reflectivity.** The knowledge of the reflectivity $R(\lambda)$ of the mirror is a prerequisite for accurate quantitative measurements based on Eq.(1). The value of $R(\lambda)$ can be determined either using the known Rayleigh scattering cross sections of gas (like He and $N_2$),[34] or using the known absorption cross sections of gas (like $NO_2$).[35-37] In this experiment, the mirror reflectivity $R(\lambda)$ was determined using the known concentration (360 ppb) $NO_2$ based on Eq. (1).

Figure 3(a) shows the observed intensities $I_0(\lambda)$ with $N_2$ and $I(\lambda)$ with 360 ppbv $NO_2$ diluted in pure $N_2$ from a reference gas cylinder inside the cavity, respectively. Given the optical cavity length of $d = 20.5$ cm, the Rayleigh scattering of $N_2$ $\alpha_{Ray,N2}(\lambda) = 7.00\times10^{-5}$ m$^{-1}$ at 293.5 K and 1 atm,[38] $\sigma_{NO2}(\lambda) = \sim 4\times10^{-19}$ cm$^2$·mol$^{-1}$ at 450 nm [39] and $n_{NO2} = 6.50\times10^{13}$ molecule/cm$^3$ for 360

ppbv $NO_2$ at 293.5 K and 1 atm, the experimental curve of $R(\lambda)$ was obtained by fitting the experimental data to :

$$\alpha_{abs,gas}(\lambda) = n_{NO2}\cdot\sigma_{NO2} + \alpha_{baseline}(\lambda) \qquad (4)$$

as plotted in Figure 3(b) upper panel. A third-order polynomial was fitted to the experimental curve to obtain an analytical expression of $R(\lambda)$. The mirror reflectivity at 450 nm was experimentally determined to be 99.99513±0.00006%, in consistency with the manufacturer's specification. The uncertainty was referred to the standard deviation of the residual (Figure 3(b) lower panel) between the experimental curve and the fit value of $R(\lambda)$.

The middle panel of Figure 3(b) presents a typical experimental BBCEAS spectrum (black line) of 360 ppbv $NO_2$ in the cavity and the corresponding fit (red line). A minimum detectable concentration of ~5.8 ppbv was deduced from the standard deviation $(4.0\times10^{-8}$ cm$^{-1})$ of the fit residuals shown in the lower panel of Figure 3(b).
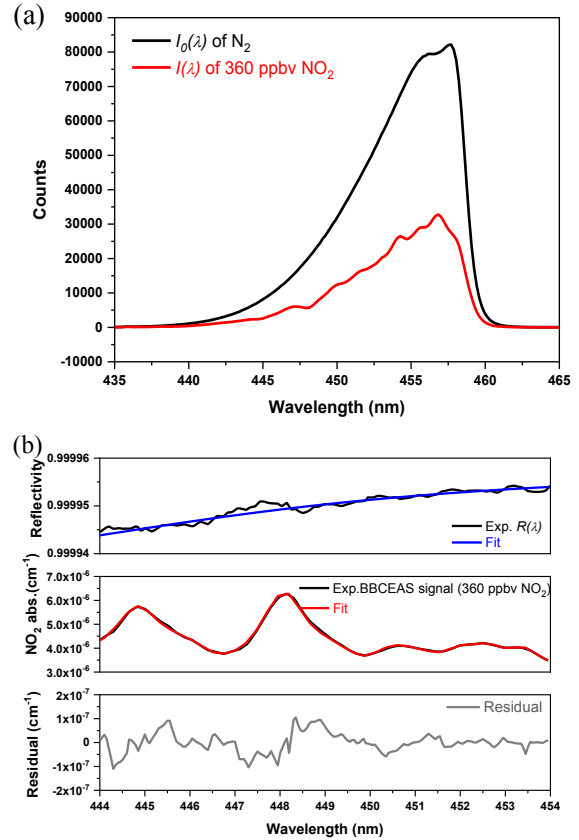


**Figure 3** (a) Light intensities $I_0(\lambda)$ and $I(\lambda)$ leaking from the cavity without and with absorbing gas (360 ppbv $NO_2$), respectively. (b) Upper panel: Experimental mirror reflectivity (black) and its fit (blue). Middle panel: Typical experimental light absorption coefficient (black) of 360 ppbv $NO_2$ and its fit (red). Lower panel: Residual (grey) between the measurement and the fit, with a standard deviation of $4.0\times10^{-8}$ cm$^{-1}$.

RESULTS AND DISCUSSION

**Detection limit and stability.** The fluctuation in incident light intensity, the spectral shift of the light source and the dark current in the spectrometer are the major factors that limit the sensitivity and stability of BBCEAS. The dependency of the detection limit on the spectral light power was experimentally evaluated. The

maximum power of the SC source used can be set at 4 W with a power density of about 1-10 mW/nm. The detection limit ($1\sigma$) of $NO_2$ was evaluated from the standard deviation (SD) of the time series measurement of $N_2$ (zero $NO_2$) at an integration time of 1 s. [27] Figure 4(a) plots the time series measurements of $NO_2$ (zero $NO_2$ in $N_2$) at different SC powers with an acquisition time of 1 s. The detection limits at 1 s integration time with different injection light powers was presented in Table 1. One could note that, with the light power of 28 µW, a $1\sigma$ detection limit of 4.61 ppbv (the SD of the black line in Figure 4(a)) was obtained with an average time of 1 s. The lowest detection limit of 0.37 ppbv (the SD of red line in Figure 4(a)) in 1 s was achieved with the light power injection of 1840 µW.

Table 1. Summary of detection limit at 1s (deduced from the standard deviation of sampling points), the optimal integration time, as well as the corresponding Allan deviation at 1s and at the optimal integration time with different light powers (28, 243, 900, and 1840 µW, respectively).

| Injection light power (µW) | 28 | 243 | 900 | 1840 |
|---|---|---|---|---|
| Detection limit (pptv) (1 s) | 4610 | 740 | 490 | 370 |
| Allan deviation (pptv) at 1s | 4620 | 680 | 350 | 290 |
| Optimal averaging time, $\tau_{opt}$ (s) | 400 | 42 | 40 | 40 |
| Allan deviation (pptv) at $\tau_{opt}$ | 150 | 113 | 70 | 60 |

The Allan deviation analysis was performed to evaluate the stability of the BBCEAS sensor operating with different injected light powers. Figure 4(b) plots the Allan deviation of the time series measurements shown in Figure 4(a) versus the average time. A minimum Allan deviation of 0.06 ppbv for $NO_2$ is achieved at 40 s integration time with a light power injection of 1840 µW. The BBCEAS has a longer stabilization time (~ 400 s) at lower light power (~ 28 µW) with respect to that at higher power (the optimal averaging time of 40 s for light powers is more than 243 µW). This is mainly due to the unstable dark current, spectral drift and in particular the power fluctuation in the SC emission because of the broadband noise resulting from quantum noise in microstructure fiber.[40] M. Islam et al. (2013) have characterized the performance of a SC source in comparison with a laser driven light source (LDLS),[41] the authors concluded that a BBCEAS system using a SC has an Allan variance's optimal integration time $\tau_{optimal}$ = 50 s, which is close to our experiment result.
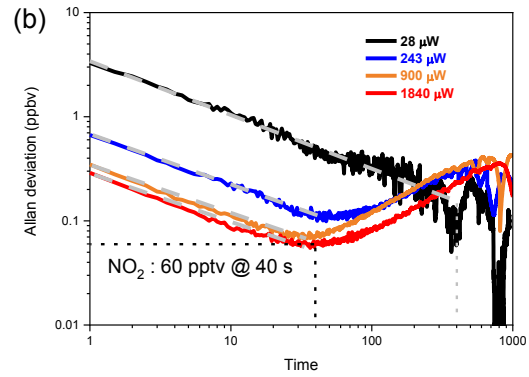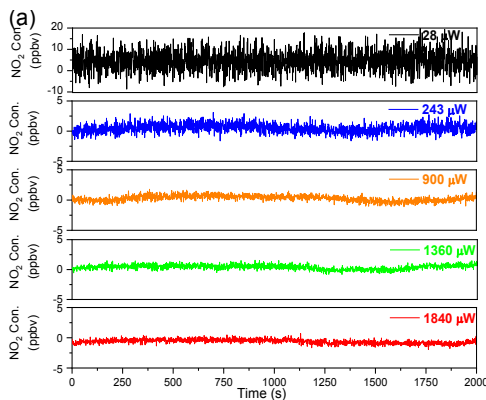




**Figure 4** (a) Time series measurements with different light powers (injected to the cavity): 28 µW (black), 243 µW (blue), 900 µW (orange), 1360 µW (green), and 1840 µW (red). (b) Allan deviation plot vs. averaging (integration) time.

In the present work, the SC power of 1840 µW was injected into the BBCEAS cavity. The instrumental performance was tested by measuring the sample of indoor air in comparison with the commercial NOx analyzer and the optical particle counter. The indoor $NO_2$ concentration, which was monitored by the NOx analyzer (AC-31M) to be constantly around 10.52 ±0.10 ppbv within 30 mins, as shown in Figure 5(a). The mass concentrations of indoor PM1, PM2.5, and PM 10 measured by OPC-N2 were constant to be around 0.034 ± 0.045 µg/m³, 0.050 ± 0.129 µg/m³, and 0.263 ± 4.580 µg/m³, respectively. Figures 5(a) and (b) show the retrieved $NO_2$ concentrations and PM extinction by BBCEAS, respectively. The Allan deviation curves in Figure 5 (c) and (d) indicate an optimum sensing performance of the BBCEAS instrument: the minimum Allan deviations (0.07 ppbv for $NO_2$ and 0.27 Mm$^{-1}$ for PM at 450 nm, respectively) are obtained with optimum averaging (integration) time of 40 s and 15 s for $NO_2$ and PM extinction, respectively. The optimal average time was longer for $NO_2$ than that for PM, so the determination of the PM extinction coefficient seems to be more sensitive to the system drift in the baseline of the BBCEAS instrument. Measurement limits ($1\sigma$) were experimentally determined to be 230 pptv at the optimum averaging time of 40 s for $NO_2$ and 1.24 Mm$^{-1}$ at the optimum averaging time of 15 s for PM extinction, respectively.
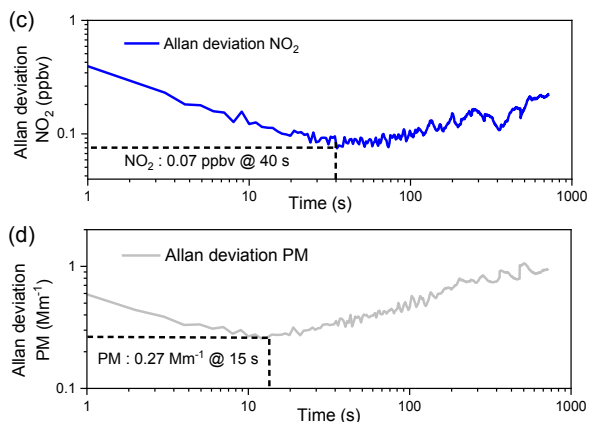


4
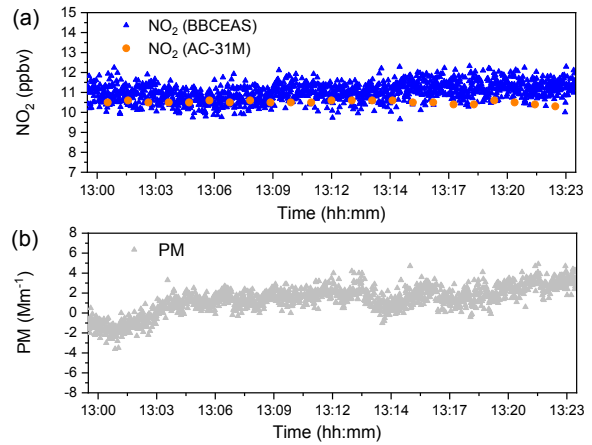
**Figure 5** Time series simultaneous measurements of $NO_2$ concentration using BBCEAS and NOx analyzer AC-31M (a) and PM light extinction (b) in indoor air. Allan variance plots of the $NO_2$ measurement (c) and PM measurement (d) showing the instrument stability induced optimal integration time of 40 s for $NO_2$ and 15 s for PM, respectively.

**Accuracy and precision.** Figures 6(a) and (b) show the distribution histogram of the retrieved $NO_2$ concentrations with $N_2$ and with 360 ppbv $NO_2$ in the cavity, accompanied with Gaussian profile fits. The value of the mean concentration of 0.41 ppbv $NO_2$ (Figure 6(a)) obtained from the measurement of zero $NO_2$ inside the cavity results in a measurement accuracy of 0.41 ppbv while the measurement precision was deduced to be 0.70 ppbv (with an average time of 1 s) from the FWHM of the fitted Gaussian profile. Based on Figure 6(b) with the measurement of 360 ppbv $NO_2$, a measurement accuracy of 5.2 ppbv was obtained with a precision of 6.58 ppbv.

**Measurement uncertainty.** The measurement uncertainty of the retrievals is mainly limited by the uncertainties of the Raylegh scattering cross section of nitrogen, the $NO_2$ absorption cross section, the light intensity $\Delta I//I$, (1-$R$) term in Eq. (6) and the statistical uncertainty of the fit.[42] The uncertainty in the determination of the (1- $R$) term using 360 ppbv $NO_2$ was estimated to be ~ 3.7 % considering the uncertainties in the used cross section of $NO_2$ (3.2 %),[37] while the uncertainty of the Raylegh scattering cross section for nitrogen (1%),[38] $\Delta I//I$ (0.8%) and the statistical uncertainty from the fit (1.4 %). The total calculated uncertainty for $NO_2$ is 5 % using the standard uncertainty propagation.



(a) Concentration distribution / Gauss fitting / Mean Con.: 0.41 ppbv / FWHM : 0.70 ppbv
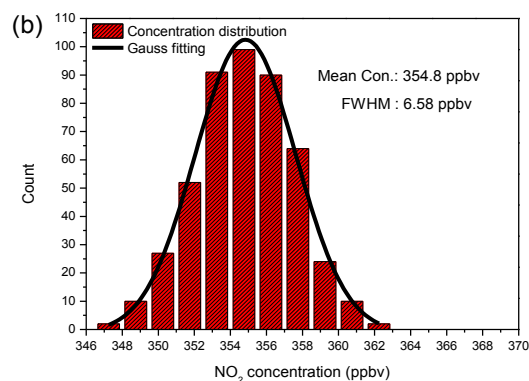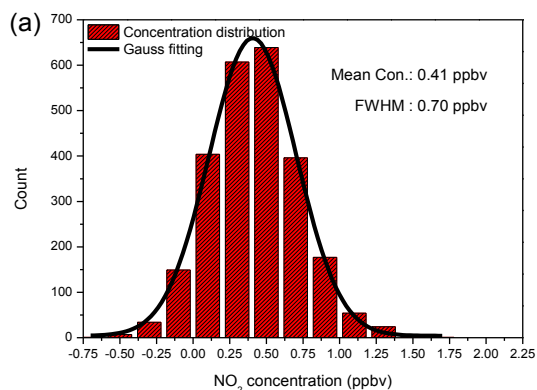


**Figure 6** Histogram showing the distribution of the estimated 0 ppbv (a) and 360 ppbv (b) $NO_2$ using the developed BBCEAS. FWHM: Full width half maximum.

**Simultaneous Measurements of PM and $NO_2$**

Simultaneous measurements of PM and $NO_2$ by the BBCEAS instrument was tested and validated by recording an episode of incense burning under laboratory conditions. The incense burning is a common ceremonial practice in religious worship, which emits gases and PM including VOCs, PM1, PM2.5, and PM10.[43,44]

A representative data retrieval of the PM extinction and the $NO_2$ concentration from the incense burning is shown in Figure 7. Indoor $NO_2$ concentration of 15 ppbv and PM extinction coefficient of 134 $Mm^{-1}$ at 450 nm from incense burning were determined by the BBCEAS with the experimental BBCEAS spectrum (black) and its fit (red) in Figure 7. Based on the SD of $6.4 \times 10^{-9}$ $cm^{-1}$ from the fit residual (grey) in Figure 7, the $1\sigma$ detection limit for $NO_2$ was deduced to be 0.9 ppbv at average time of 1 s. The PM extinction detection limit at 1 s was determined to be 1.41 $Mm^{-1}$ retrieved from the SD of the BBCEAS signals with non-particulate sample flashing in the cavity.
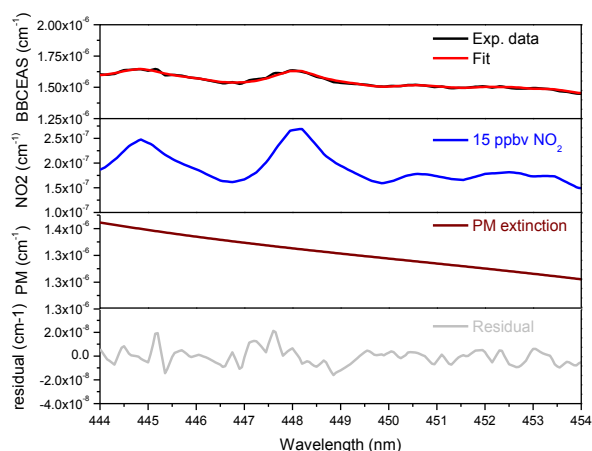


**Figure 7** Typical experimental BBCEAS spectrum (black) accompanied with its fit (red), decomposed absorption spectrum of 15 ppbv $NO_2$ (blue) and PM extinction coefficient of 134 $Mm^{-1}$. The residual (grey) between the measurement and the fit results in a standard deviation of $6.4 \times 10^{-9}$ $cm^{-1}$.

Time-series measurements of PM from incense burning and indoor $NO_2$ are shown in Figures 8(a) and (c), respectively. The duration of incense burning for one stick was around 40 minutes.

The baselines of the BBCEAS were checked every 5 minutes by flushing the cavity with $N_2$ and used for the determination of PM extinction. Figure 8(a) (upper panel) shows the measured PM extinction coefficient (black) by BBCEAS at 450 nm with an acquisition time of 1 s (4 spectra averaging with 250 ms integration time per spectrum), the measured PM1 (Middle panel) by OPC-N2 sampling at a rate of 1 s. As shown in Figure 8 (a) bottom panel, the instrumental baseline was regularly checked every 5 min with nitrogen passing through the cavity. The variation ranged from -5 Mm$^{-1}$ to 5 Mm$^{-1}$ in the bottom panel of Figure 8(a), which indicates the measurement uncertainty was within ±5 Mm$^{-1}$ due to the fluctuation of the instrumental baseline in a short time scale. Several previous investigations reported that the size distribution of PM from incense burning is concentrated in ~1 μm.[45-47] The measured PM1 mass concentrations are used for comparison. As the extinction coefficient is proportional linearly to the mass concentration of the particles,[48] the correlation between the measured PM extinction coefficient from the BBCEAS (time resolution of 1 s) and the PM1 mass concentration by OPC-N2 have been investigated. Good correlation is shown in Figure 8(b) with a linear fit of $y = 90.62x + 3.16$ and a regression coefficient $r^2 = 0.91$. The PM1 data from OPC-N2 (blue) correlates better with the non-size selection measurement of PM from the BBCEAS instrument. Regarding $NO_2$ measurement (time resolution of 1 min), a good linear correlation between the $NO_2$ concentrations measured by BBCEAS and by AC-31M was obtained with a $r^2=0.94$, as shown in Figure 8 (d).
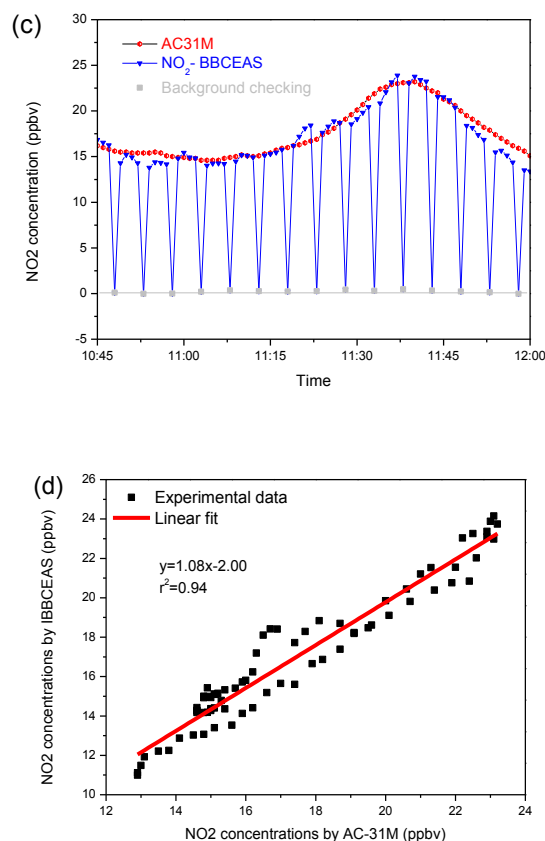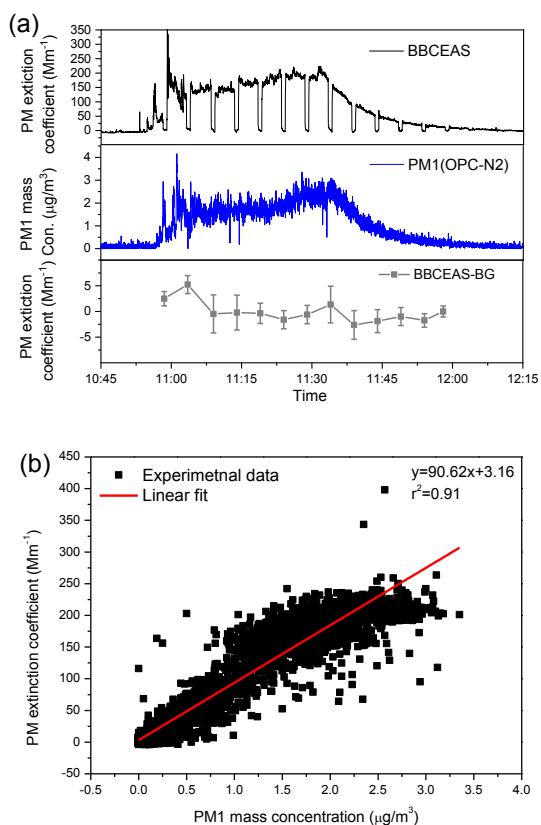


(a)



(b)



(c)



(d)

**Figure 8** (a) Time series measurements of the PM extinction by BBCEAS at 450 nm (black) as well as the PM1 mass concentrations measured by the OPC-N2 (blue for PM1) at a sampling rate of 1 s. The BBCEAS baseline was checked every 5 min and used for the determination of PM extinction. (b) Correlation plot of the PM extinction coefficient (at 450 nm) against the PM1 mass concentration. (c) Indoor $NO_2$ concentration measurements using the AC-31 M (red) and the BBCEAS (blue) during the incense burning. Time series of the $N_2$ extinction (Grey) was recorded to check the background drift every 5 minutes. (d) Correlation of indoor $NO_2$ concentrations measured by BBCEAS vs. AC 31M.

## Conclusions

Simultaneous measurements of the trace gas and particulate matter are of great interesting for environmental monitoring of air quality. A newly developed BBCEAS instrument for simultaneous measurement of $NO_2$ and particulate matter is reported with a novel scheme with real time correction of background baseline for accurately measurement of the PM extinction. The BBCEAS instrument was operated in the spectral region of 444-460 nm using a supercontinuum source, which performance was tested by side-by-side continuous measurement of indoor $NO_2$ with a reference NOx analyzer. Simultaneous measurements of $NO_2$ and PM were performed during an incense burning. Measurement limits (1σ) were experimentally determined to be 230 pptv in 40 s for $NO_2$ and 1.24 Mm$^{-1}$ for PM (extinction coefficient) in 15 s, respectively.

PM measurements by BBCEAS at 450 nm and by an OPC-N2 counter were linearly correlated with a regression coefficient $r^2 = 0.91$. $NO_2$ concentrations measured by BBCEAS and by a reference NOx analyzer showed a good linear correlation with $r^2 =$

0.94. This laboratory test has demonstrated the feasibility of BBCEAS for simultaneous measurements of PM and $NO_2$ in the atmosphere, which can be extended to simultaneous measurements of PM extinction and other atmospheric gaseous species.

In addition, the dependence of the instrument detection limit on the input light power in the BBCEAS instrument using a supercontinuum light source is investigated in this paper. It was observed that higher light intensity injected to the cavity resulted in a lower detection limit, while the instrument stabilization time became shorter (shorter optimal integration time). Supercontinuum light source offers laser like output properties, which efficiently improve the light-cavity coupling efficiency: a few mW compared to hundreds mW from a LED with similar detection limit.[23,37,49] For future work, the BBCEAS instrument performance can be further improved using a light source with higher power and longer-time stability.

## ASSOCIATED CONTENT

### Supporting Information

The Supporting Information is available free of charge on the ACS Publications website.

Transmission spectra of the specific filter set used in the BBCEAS system (PDF).

## AUTHOR INFORMATION

### Corresponding Author

Qian Gou - School of Chemistry and Chemical Engineering, Chongqing University, Daxuecheng South Rd. 55, 401331 Chongqing, China; ORCID: 0000-0003-3831-3582; Email: qian.gou@cqu.edu.cn

Weidong Chen - Laboratoire de Physicochimie de l'Atmosphère, Université du Littoral Côte d'Opale, 189A Avenue Maurice Schuman, 59140 Dunkerque, France; ORCID: 0000-0001-6141-1039; Email:weidong.chen@univ-littoral.fr

### Authors

Gaoxuan Wang - Ningbo research institute, Zhejiang University, Qianhu south road Rd.1, 315100 Ningbo, China; ORCID: 0000-0003-3243-3145; Email: gaoxuanwang@zju.edu.cn

Lingshuo Meng - Laboratoire de Physicochimie de l'Atmosphère, Université du Littoral Côte d'Opale, 189A Avenue Maurice Schuman, 59140 Dunkerque, France; Email: menglingshuo@126.com

Benjamin Hanoune - Physicochimie des Processus de Combustion et de l'Atmosphère, Université Lille1 Sciences et Technologies, Bâtiment C11, 59655 Villeneuve d'Ascq, France; Email: benjamin.hanoune@univ-lille1.fr

Suzanne Crumeyrolle - Laboratoire d'Optique Atmosphérique, Université de Lille1, Bâtiment P5, 59655 Villeneuve d'Ascq, France; Email: suzanne.crumeyrolle@univ-lille.fr

Thomas Fagniez - Laboratoire de Physicochimie de l'Atmosphère, Université du Littoral Côte d'Opale, 189A Avenue Maurice Schuman, 59140 Dunkerque, France; Email: Thomas.Fagniez@univ-littoral.fr

Cécile Coeur - Laboratoire de Physicochimie de l'Atmosphère, Université du Littoral Côte d'Opale, 189A Avenue Maurice Schuman, 59140 Dunkerque, France; Email: cecile.coeur@univ-littoral.fr

Rony Akiki - ENVEATM (ex Environment SA), 111 Boulevard Robespierre CS 80004, 78304 Poissy Cedex 4, France; r.akiki@environnement-sa.com

## Notes

The authors declare no competing financial interest.

## REFERENCE

[1]. Monks, P.; Granier, C.; Fuzzi, S.; Stohl, A.; Williams, M.; Akimoto, H.; Amann, M.; Baklanov, A.; Baltensperger, U.; Bey, I. Atmospheric composition change–global and regional air quality, Atmos. Environ. **2009**, 43, 5268-5350.

[2]. Kelly, F. J.; Fussell, J. C. Size, source, and chemical composition as determinants of toxicity attributable to ambient particulate matter, Atmos. Environ. **2012**, 60, 504-526.

[3]. Kinney, P. L. Interactions of Climate Change, Air Pollution, and Human Health, Curr. Env. Heal. Rep., **2018**, 5,179–186.

[4]. Rajagopalan, S.; Al-Kindi, S. G.; Brook, R. D. Air Pollution and Cardiovascular Disease, J. Am. Coll. Cardiol. **2018**, 72, 2054-2070.

[5]. Moise, T.; Flores, J. M.; Rudich, Y. Optical Properties of Secondary Organic Aerosols and Their Changes by Chemical Processes, Chem. Rev. **2015**, 115, 4400–4439.

[6]. Beckermana, B.; Jerrettb, M.; Brookd, J. R.; Vermae, D. K.; Araine, M. A.; Finkelsteine, M. M. Correlation of nitrogen dioxide with other traffic pollutants near a major expressway, Atmos. Environ. **2008**, 42, 275–290.

[7]. Chen, W.; Venables, D. S. Broadband optical cavity methods. **2021**, 95-158.

[8]. Popa, D.; Udrea, F. Towards Integrated Mid-Infrared Gas Sensors. Sensors, **2019**, 19, 9.

[9]. Moosmüller, H.; Chakrabarty, R. K.; Arnott, W. P. Aerosol light absorption and its measurement: a review, J. Quant. Spectrosc. Rad. Transfer., **2009**, 110, 844–878.

[10]. Cotterell, M. I.; Knight, J. W.; Reid, J. P.; Orr-Ewing, A. J. Accurate Measurement of the Optical Properties of Single Aerosol Particles Using Cavity Ring-Down Spectroscopy, J. Phys. Chem. A. **2022**, 126, 2619–2631.

[11]. Varma, R.; Moosmüller, H.; Arnott, W. P. Toward an ideal integrating nephelometer, Opt. Lett. **2003**, 28, 1007-1009.

[12]. Weingartner, E.; Saathoff, H.; Schnaiter, M.; Streit, N.; Bitnar, B.; Baltensperger, U. Absorption of light by soot particles: determination of the absorption coefficient by means of aethalometers, J. Aerosol Sci. **2003**, 34, 1445-1463.

[13]. Ajtai, T.; Filep, Á.; Kecskeméti, G.; Hopp, B.; Bozóki, Z.; Szabó, G. Wavelength dependent mass-specific optical absorption coefficients of laser generated coal aerosols determined from multi-wavelength photoacoustic measurements, Appl. Phys. A, **2011**, 103,1165-1172.

[14]. Lack, D. A.; Richardson, M. S.; Law, D.; Langridge, J. M.;

Cappa, C. D.; McLaughlin, R. J.; Murphy, D. M. Aircraft instrument for comprehensive characterization of aerosol optical properties, Part 2: Black and brown carbon absorption and absorption enhancement measured with photo acoustic spectroscopy, Aerosol Sci. Tech. **2012**, 46, 555-568.

[15]. Wang, G.; Kulinski, P.; Hubert, P.; Deguine, A.; Petitprez, D.; Crumeyrolle, S.; Fertein, E.; Deboudt, K.; Flament, P.; Sigrist, M. W.; Yi, H.; Chen, W. Filter-Free Light Absorption Measurement of Volcanic Ashes and Ambient Particulate Matter Using Multi-Wavelength Photoacoustic Spectroscopy, Prog. Electromagn. Res. **2019**, 166, 59-74.

[16]. Schnaiter, M.; Schmid, O.; Petzold, A.; Fritzsche, L.; Klein, K. F.; Andreae, M. O.; Helas, G.; Thielmann, A.; Gimmler, M.; Möhler, O.; Linke, C.; Schurath, U. Measurement of Wavelength-Resolved Light Absorption by Aerosols Utilizing a UV-VIS Extinction Cell, Aerosol Sci. Tech. **2005**, 39, 249-260.

[17]. Chartier, R. T.; Greenslade, M. E. Initial investigation of the wavelength dependence of optical properties measured with a new multi-pass Aerosol Extinction Differential Optical Absorption Spectrometer (AE-DOAS), Atmos. Meas. Tech. **2012**, 5, 709-721.

[18]. Lack, D. A.; Moosmüller, H.; McMeeking, G. R.; Chakrabarty, R. K.; Baumgardner, D. Characterizing elemental, equivalent black, and refractory black carbon aerosol particles: a review of techniques, their limitations and uncertainties, Anal. Bioanal Chem. **2014**, 406, 99–122.

[19]. Miklós, A.; Hess, P.; Bozóki, Z. Application of acoustic resonators in photoacoustic trace gas analysis and metrology. Rev. Sci. Instrum. **2001**, 72, 1937–1955.

[20]. Bluvshtein, N.; Flores,J. M.; Segev, L.; Rudich, Y. A new approach for retrieving the UV–vis optical properties of ambient aerosols, Atmos. Meas. Tech. **2016**, 9, 3477–3490.

[21]. Strawa, A. W.; Castaneda, R.; Owano, T.; Baer, D. S.; Paldus, B. A. The measurement of aerosol optical properties using continuous wave cavity ring-down techniques, J. Atmos. Ocean. Tech. **2003**, 20, 454-465.

[22]. Massoli, P.; Kebabian, P. L.; Onasch, T. B.; Hills, F. B.; Freedman, A. Aerosol light extinction measurements by cavity attenuated phase shift (CAPS) spectroscopy: Laboratory validation and field deployment of a compact aerosol particle extinction monitor, Aerosol Sci. Tech. **2010**, 44, 428-435.

[23]. Washenfelder, R. A.; Flores, J. M.; Brock, C. A.; Brown, S. S.; Rudich, Y. Broadband measurements of aerosol extinction in the ultraviolet spectral region Atmos. Meas. Tech. **2013**, 6, 861–877.

[24]. Zhao, W.; Xu, X.; Dong, M.; Chen, W.; Gu, X.; Hu, C.; Huang, Y.; Gao, X.; Huang, W.; Zhang, W. Development of a cavity-enhanced aerosol albedometer, Atmos. Meas. Tech. **2014**, 7, 2551–2566.

[25]. Baynard, T.; Lovejoy, E. R.; Pettersson, A.; Brown, S. S.; Lack, D.; Osthoff, H.; Massoli, P.; Ciciora, S.; Dube, W.P.; Ravishankara, A. R. Design and application of a pulsed cavity ring-down aerosol extinction spectrometer for field measurements, Aerosol Sci. Tech. **2007**, 41, 447–462.

[26]. Yu, Z.; Ziemba, L. D.; Onasch, T. B.; Herndon, S. C.; Albo, S. E.; Miake-Lye, R.; Anderson, B. E.; Kebabian, P. L.; Freedman, A. Direct measurement of aircraft engine soot emissions using a cavity-attenuated phase shift (CAPS)-based extinction monitor, Aerosol Sci. Tech.

**2011**, 45, 1319-1325.

[27]. Zhao, W.; Dong, M.; Chen, W.; Gu, X.; Hu, C.; Gao, X.; Huang, W.; Zhang, W. Wavelength-resolved optical extinction measurements of aerosols using broad-band cavity-enhanced absorption spectroscopy over the spectral range of 445−480 nm, Anal. Chem. **2013**, 85, 2260−2268.

[28]. Varma, R. M.; Venables, D. S.; Ruth, A. A.; Heitmann, U.; Schlosser, E.; Dixneuf, S. Long optical cavities for open-path monitoring of atmospheric trace gases and aerosol extinction, Appl. optics, **2009**, 48, B159-B171.

[29]. Varma, R. M.; Ball,S. M.; Brauers, T.; Dorn, H. P.; Heitmann, U.; Jones, R. L.; Platt, U.; Pöhler, D.; Ruth, A. A.; Shillings, A. J. L.; Thieser, J.; Wahner, A.; Venables, D. S. Light extinction by secondary organic aerosol: an intercomparison of three broadband cavity spectrometers, Atmos. Meas. Tech. **2013**, 6, 3115-3130.

[30]. Weiden, S. L.; Drewnick, F.; Borrmann, S. Particle Loss Calculator – a new software tool for the assessment of the performance of aerosol inlet systems, Atmos. Meas. Tech. **2009**, 2, 479–494.

[31]. Kebabian, P. L.; Wood, E. C.; Herndon, S. C.; Freedman, A. A Practical Alternative to Chemiluminescence-Based Detection of Nitrogen Dioxide: Cavity Attenuated Phase Shift Spectroscopy, Environ. Sci. Technol. **2008**, 42, 6040–6045.

[32]. Platt, U.; Meinen, J.; Pöhler, D.; Leisner, T. Broadband cavity enhanced differential optical absorption spectroscopy (CE-DOAS)-applicability and corrections, Atmos. Meas. Tech. **2009**, 2, 713–723.

[33]. Thalman, R.; Volkamer, R. Inherent calibration of a blue LED-CE-DOAS instrument to measure iodine oxide, glyoxal, methyl glyoxal, nitrogen dioxide, water vapour and aerosol extinction in open cavity mode, Atmos. Meas. Tech. **2010**, 3, 1797–1814.

[34]. Washenfelder, R.; Langford, A.; Fuchs, H.; Brown, S. Measurement of glyoxal using an incoherent broadband cavity enhanced absorption spectrometer, Atmos. Chem. Phys. **2008**, 8, 7779-7793.

[35]. Gherman, T.; Venables, D. S.; Vaughan, S.; Orphal, J.; Ruth, A. A. Incoherent broadband cavity-enhanced absorption spectroscopy in the near-ultraviolet: Application to HONO and $NO_2$, Environ. Sci. Technol. **2007**, 42, 890-895.

[36]. Wu, T.; Tourneur, C. C.; Dhont, G.; Cassez, A.; Fertein, E.; He, X.; Chen, W. Simultaneous monitoring of temporal profiles of $NO_3$, $NO_2$ and $O_3$ by in coherent broadband cavity enhanced absorption spectroscopy for atmospheric applications, J. Quant. Spectrosc. Rad. Transfer. **2014**, 133, 199–205.

[37]. Yi, H.; Wu, T.; Wang, G.; Zhao, W.; Fertein, E.; Coeur, C.; Gao, X.; Zhang, W.; Chen, W. Sensing atmospheric reactive species using light emitting diode by incoherent broadband cavity enhanced absorption spectroscopy, Opt. express, **2016**, 24, A781-790.

[38]. Sneep, M.; Ubachs, W. Direct measurement of the Rayleigh scattering cross section in various gases, J. Quant. Spectrosc. Rad. Transfer. **2005**, 92, 293-310.

[39]. Bogumil, K.; Orphal, J.; Homann, T.; Voigt, S.; Spietz, P.; Fleischmann, O.; Vogel, A.; Hartmann, M.; Kromminga, H.; Bovensmann, H. Measurements of molecular absorption spectra with the SCIAMACHY pre-flight model: instrument characterization and reference data for atmospheric remote-sensing in the 230–2380 nm region, J. Photoch. Photobio. A, **2003**, 157, 167-184.

[40]. Corwin, K. L.; Newbury, N. R.; Dudley, J. M.; Coen, S.; Diddams, S. A.; Weber, K.; Windeler, R. Fundamental noise limitations to supercontinuum generation in micro-structure fiber, Phys. Rev. Lett. **2003**, 90, 113904.

[41]. Islam, M.; Ciaffoni, L.; Hancock, G.; Ritchie, G. A. D. Demonstration of a novel laser-driven light source for broadband spectroscopy between 170 nm and 2.1 mm, Analyst, **2013**, 138, 4741.

[42]. Wu, T.; Chen, W.; Fertein, E.; Cazier, F.; Dewaele, D.; Gao, X. Development of an open-path incoherent broad-band cavity-enhanced spectroscopy based instrument for simultaneous measurement of HONO and NO2 in ambient air, Appl. Phys. B-Lasers O. **2011**, 106, 501-509.

[43]. Kuo, S. C.; Tsai, Y. I.; Sopajaree, K. Emission characteristics of carboxylates in PM 2.5 from incense burning with the effect of light on acetate, Atmos. Environ. **2016**, 138, 125-134.

[44]. See, S. W.; Balasubramanian, R. Characterization of fine particle emissions from incense burning, Build. Environ. **2011**, 46, 1074-1080.

[45]. Goel, A.; Wathore, R.; Chakraborty, T.; Agrawal, M. Characteristics of Exposure to Particles due to Incense Burning inside Temples in Kanpur, India, Aerosol Air Qual. Res. **2017**, 17, 608–615.

[46]. Fang, G.; Chang, C.; Wu, Y.; Yang, C.; Chang, S.; Yang, I. Suspended particulate variations and mass size distributions of incense burning at Tzu Yun Yen temple in Taiwan, Taichung. Sci. Total. Environ. **2002**, 299, 79-87.

[47]. See, S.; Balasubramanian, R.; Joshi, U. M. Physical characteristics of nanoparticles emitted from incense smoke, Sci. and Technol. of Adv. Mat. **2007**, 8, 25–32.

[48]. Alexander, D.; Kokhanovsky, A. Light absorption and scattering by particles in the atmosphere, Praxis Publishing Ltd. Chichester, **2008**.

[49]. Wu, T.; Zha, Q.; Chen, W.; Xu, Z.; Wang, T.; He, X. Development and deployment of a cavity enhanced UV-LED spectrometer for measurements of atmospheric HONO and NO2 in Hong Kong, Atmos. Environ., **2014**, 95, 544-551.